Comparing Transient High-Confinement States in Spheromak and RFP Discharges

Carl Sovinec,

James Reynolds, and Giovanni Cone

University of Wisconsin-Madison

9th Easter Plasma Meeting on Stability and Confinement of Magnetized Plasmas

Torino, Italy, March 30-April 1, 2005

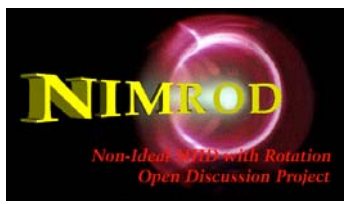

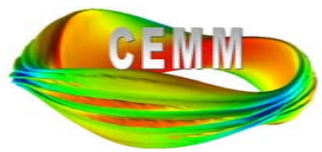

Outline

- Introduction
  - Spheromak sustainment vs. decay
  - RFP pulsed “parallel” current drive
- SSPX modeling
  - Parameters of the computations
  - Comparison with SSPX results
  - Importance of transients
- RFP PPCD modeling
  - Poloidal **E** pulse
  - Poloidal and toroidal **E** pulse
- Comparison and conclusion

Introduction

- Spheromaks
  - The previous generation of experiments achieved their highest temperatures during decay [400 eV in CTX—Jarboe, PF B **2**, 1342 (1990)].
  - SSPX finds that a second electrostatic current pulse improves performance [McLean, PRL **88**, 125004 (2002)].
  - Toroidal current and magnetic energy decay slightly during the second pulse but are not fixed, and the role of the transient is not clear from experimental evidence alone.
  - Resistive MHD simulations at 0-β have found chaotic scattering during sustainment and flux-surface formation during decay [Finn, PRL **85**, 4538 (2000) and Sovinec, PoP **8**, 475 (2001)].

Introduction (continued)

- Reversed-field Pinches
  - Efforts to reduce the free energy for tearing modes in MST found sawtooth suppression upon application of poloidal **E** (PPCD) [Sarff, PRL **72**, 3670 (1994)].
  - Refinement of the transient technique found further confinement improvement when $E_{||}(a)$ is kept positive by reducing the toroidal loop voltage [Chapman, PoP **9**, 2061 (2002)].
  - Resistive MHD simulations at 0-β have been very helpful in understanding nonlinear MHD in sustained conditions [many] and PPCD [Puiatti, NF **43**, 1057 (2003)].
- Both
  - Nonlinear simulations can be used to understand how profiles evolve and interact with MHD activity.

Simulation of SSPX 4620-4644 Shot Series

- **Detailed modeling of specific discharges started with a realistic domain.**

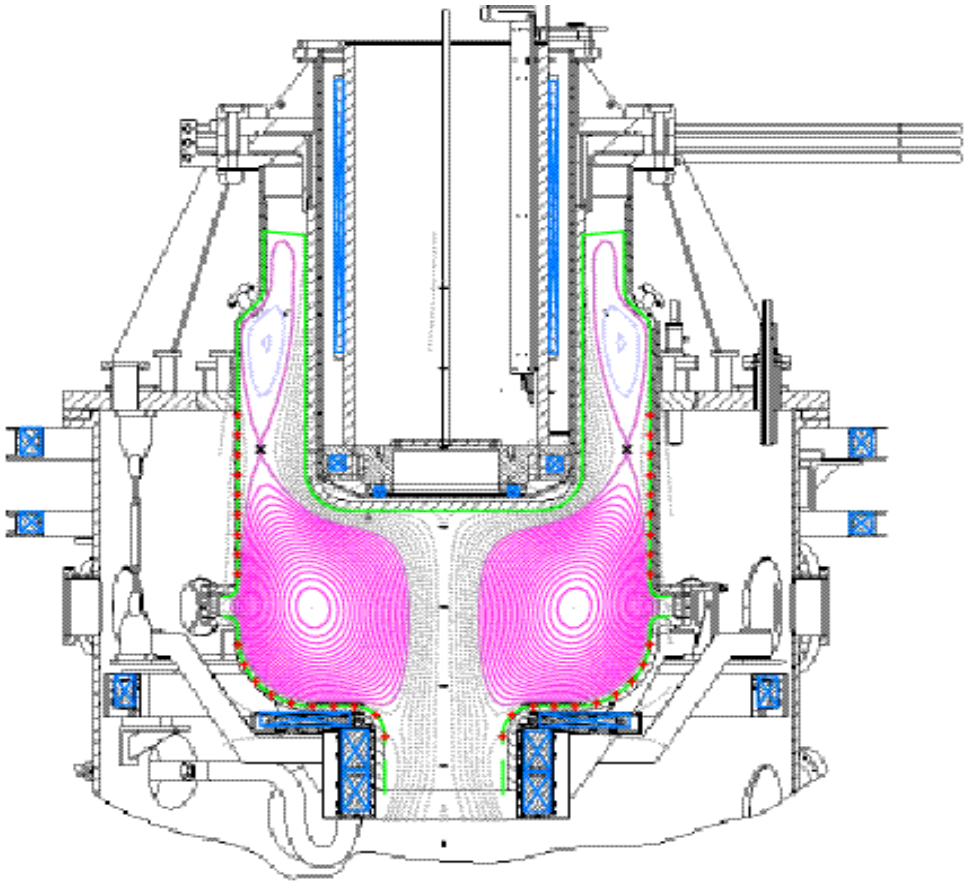

Schematic of the SSPX spheromak experiment at LLNL with contours of reconstructed symmetric poloidal flux.

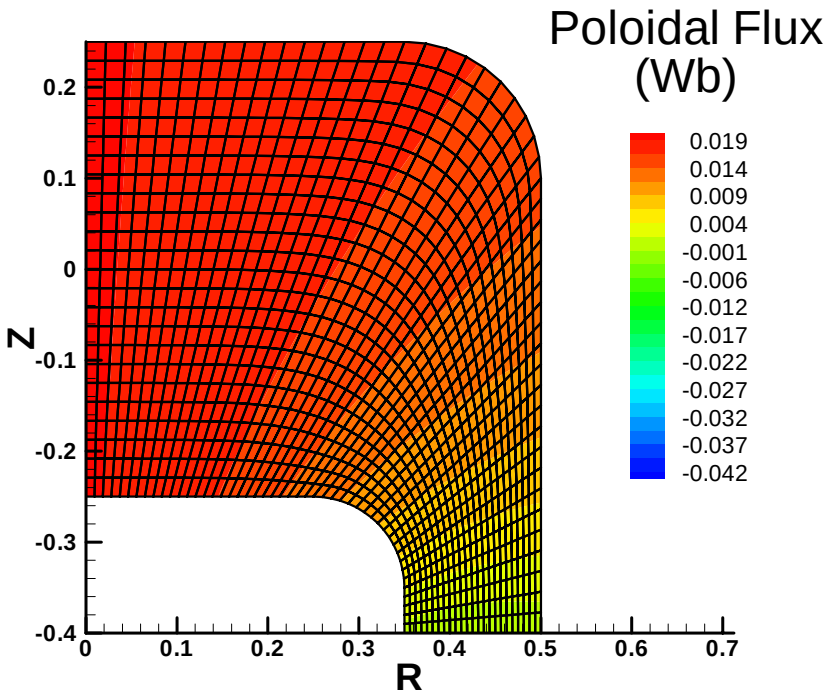

Initial (vacuum) poloidal flux distribution and the NIMROD mesh of bicubic finite elements representing SSPX (upside down).

The SSPX computations evolve temperature and number density, in addition to magnetic field and plasma flow velocity, to allow resistivity to change with temperature.

$$\frac{\partial \mathbf{B}}{\partial t} = \nabla \times \left(\mathbf{V} \times \mathbf{B} - \eta \mathbf{J} \right)$$

Faraday's/Ohm's laws

$$\mu_0 \mathbf{J} = \nabla \times \mathbf{B}$$

low-ω Ampere's law

$$\rho \left(\frac{\partial \mathbf{V}}{\partial t} + \mathbf{V} \cdot \nabla \mathbf{V} \right) = \mathbf{J} \times \mathbf{B} - \nabla p + \nabla \cdot \nu \rho \nabla \mathbf{V}$$

flow evolution

$$\frac{\partial n}{\partial t} + \nabla \cdot \left(n \mathbf{V} \right) = \nabla \cdot D \nabla n$$

particle continuity

$$\frac{n}{\gamma - 1} \left(\frac{\partial T}{\partial t} + \mathbf{V} \cdot \nabla T \right) = -\frac{p}{2} \nabla \cdot \mathbf{V} + \nabla \cdot n \left[\chi_{\parallel} \hat{\mathbf{b}} \hat{\mathbf{b}} + \chi_{\perp} \left(\mathbf{I} - \hat{\mathbf{b}} \hat{\mathbf{b}} \right) \right] \cdot \nabla T + \frac{\eta \mathbf{J}^2}{2}$$

(single) temperature evolution

$$\hat{\mathbf{b}} \equiv \mathbf{B} / |\mathbf{B}|$$

local magnetic direction vector

- Braginskii transport coefficients are used for $\chi_{\parallel}$ (electron), $\chi_{\perp}$ (ion), and η.
- Heating is Ohmic.
- The NIMROD code [http://nimrodteam.org] evolves the system in 3D.
  - High-order finite elements help resolve anisotropies [JCP **195**, 355 (2004)].

Parameters for the Computation

INPUT (Collisional coefficients are based on Hydrogen and Z=1):

- n=5×10^{19} m^{-3}
- $\frac{\eta(T)}{\mu_0} = 411\left(\frac{1\,\mathrm{eV}}{T}\right)^{3/2}$ m^2/s
- $\chi_{\parallel}(T) = 387\left(\frac{T}{1\,\mathrm{eV}}\right)^{5/2}$ m^2/s
- $\chi_{\perp} = 0.50\left(\frac{1\,\mathrm{eV}}{T}\right)^{1/2}\left(\frac{1\,\mathrm{T}}{B}\right)^{2}$ m^2/s

- T_{wall} = 0.1 eV
- ψ_{vacuum} specified
- $I_{\mathrm{inj}}(t)$ via boundary conditions on **B**
- Heat sink controls boundary layer
- ν=D=2000 m^2/s

OUTPUT: Everything else

- Notes on collisional transport:
  - At n=5×10^{19} m^{-3} and T=1 eV, $\lambda_e \cong 4\times10^{-4}$ m << L
  - Scaling λ_e with T^2 indicates that λ_e reaches the chamber radius at approximately 35 eV.
  - Collisional 3D transport modeling is appropriate for a chaotic **B** topologies if the effective mean-free-path is sufficiently small.
  - We can confirm *a posteriori* that collisionless conditions only exist when and where closed flux surfaces form.
- We infer that anisotropic thermal conduction is a good model for sustained (open field) conditions and for the transition to closed flux during decay.

Comparison of Numerical and Experimental Results

The simulated injector current is programmed to approximate the series of SSPX discharges reported in [McLean, *et al.*, PRL **88**, 125004 (2002)].

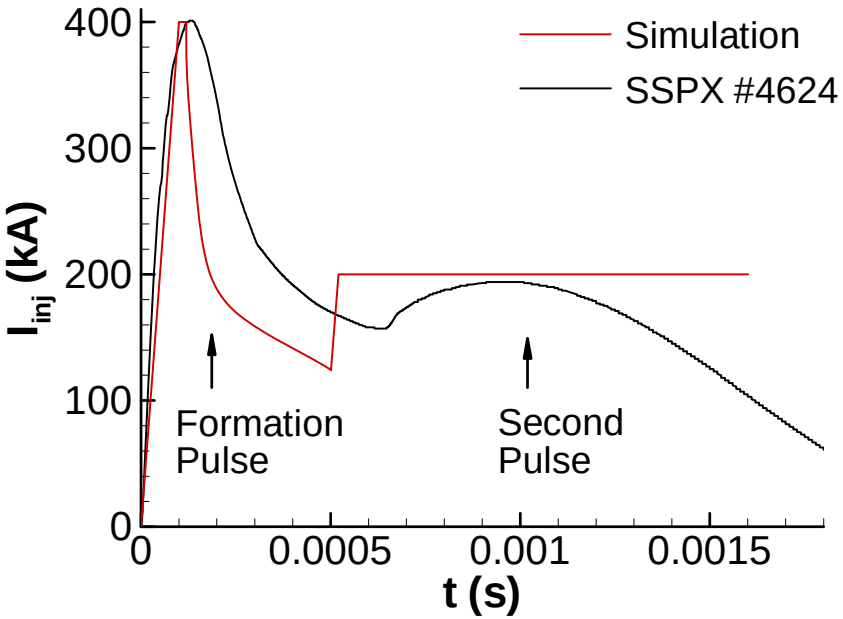

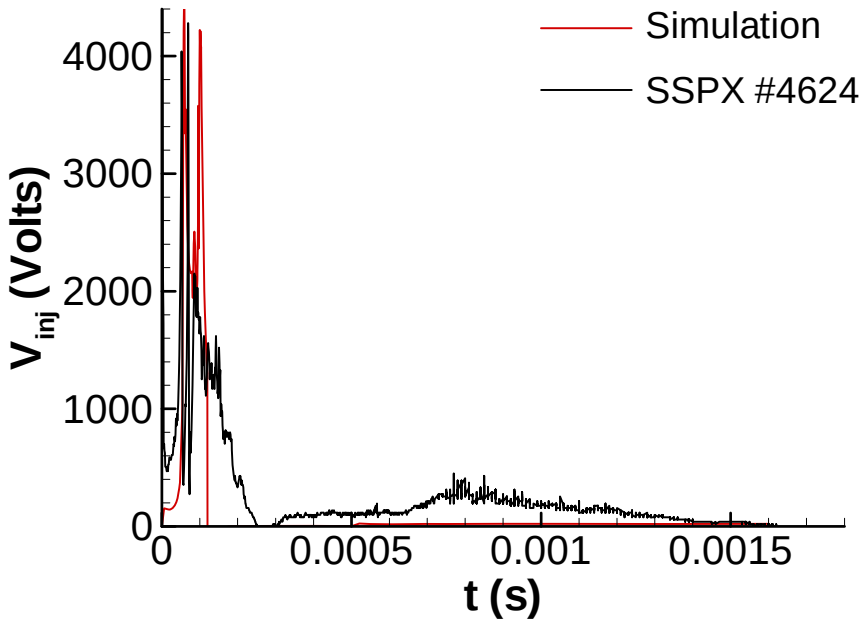

INPUT: A strongly driven phase is followed by decay and then a second, partial drive. [SSPX Data courtesy of H. S. McLean.]

During formation, the applied potential reaches a few kV. During the second pulse, the potential is ~200 V in SSPX [including 100-150 V of sheath, Hooper, Stallard] and 20 V in the simulation.

- The peak instantaneous power input reaches ~1 GW in the formation stage.

Toroidal current and magnetic energy evolution from the simulations are similar to results found by CORSICA fits to laboratory observations [Hooper *et al.*, NF **39**, 863 (1999)] during the second current pulse.

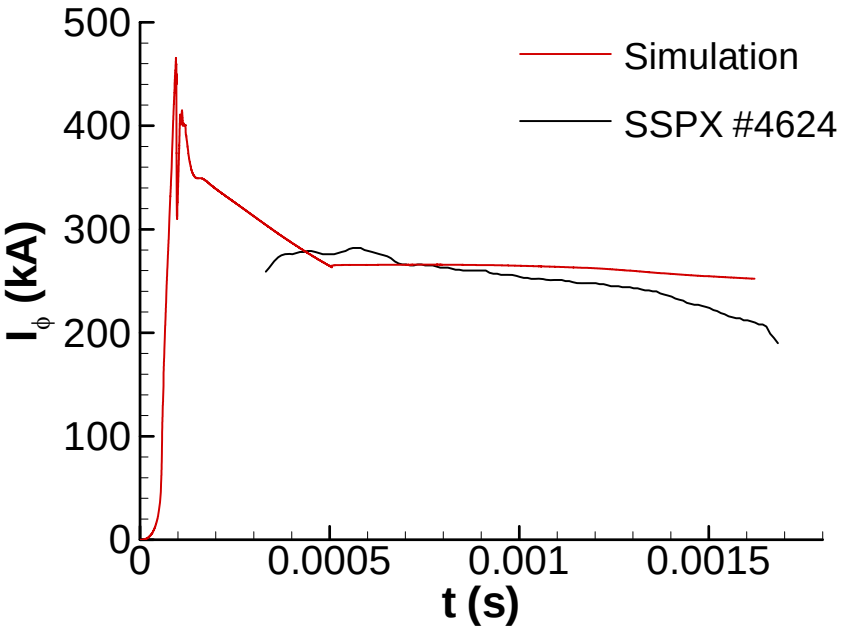

I_{tor} resulting from the series of NIMROD simulations is compared with I_{tor} from CORSICA equilibrium fits of SSPX data.

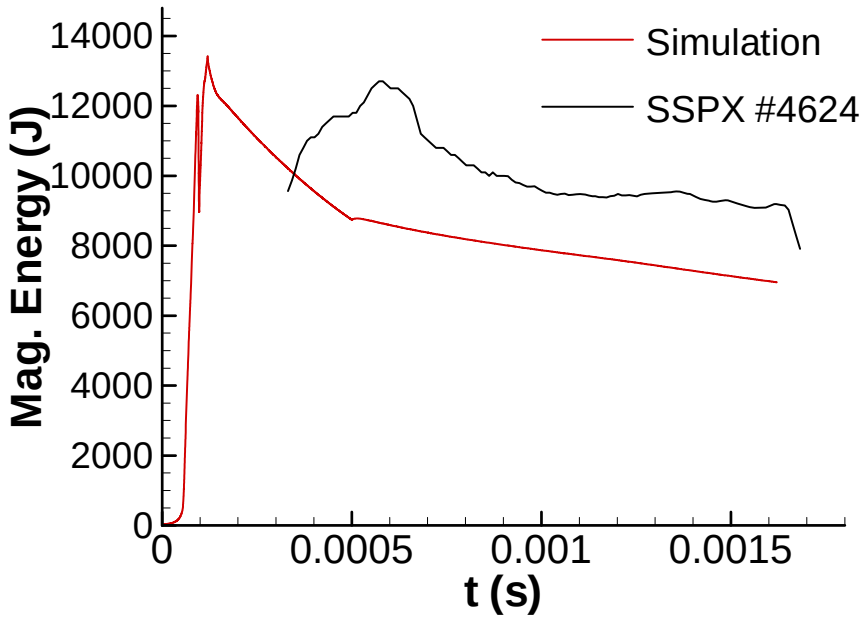

Decay of magnetic energy is slowed by the partial drive.

• In the simulation, the second current pulse provides 4 MW of power, and the decay of magnetic energy provides an additional 1.4 MW.

Both simulation and experiment show a quiescent phase when the second current pulse is applied after a brief period of decay.

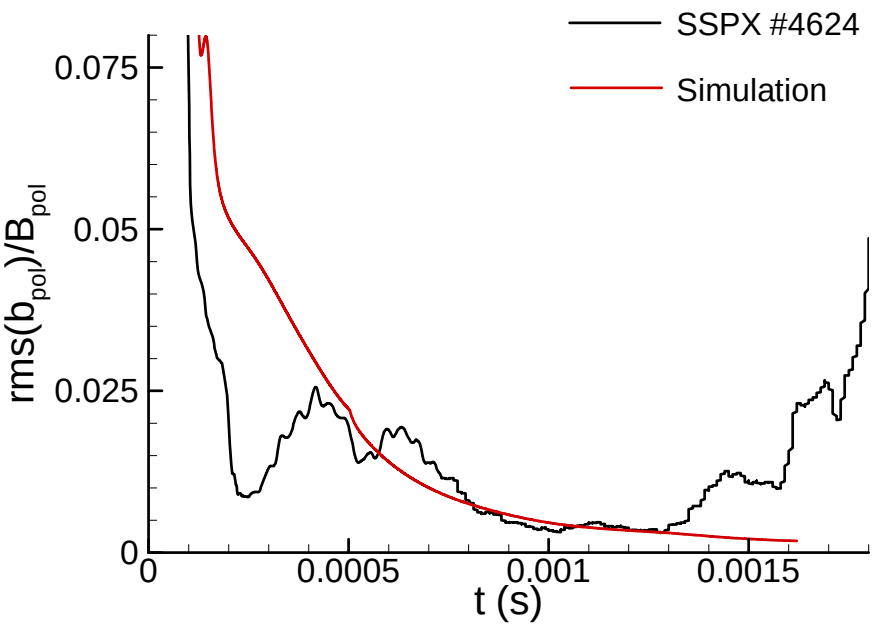

Relative poloidal magnetic field fluctuations at the outboard mid-plane position.

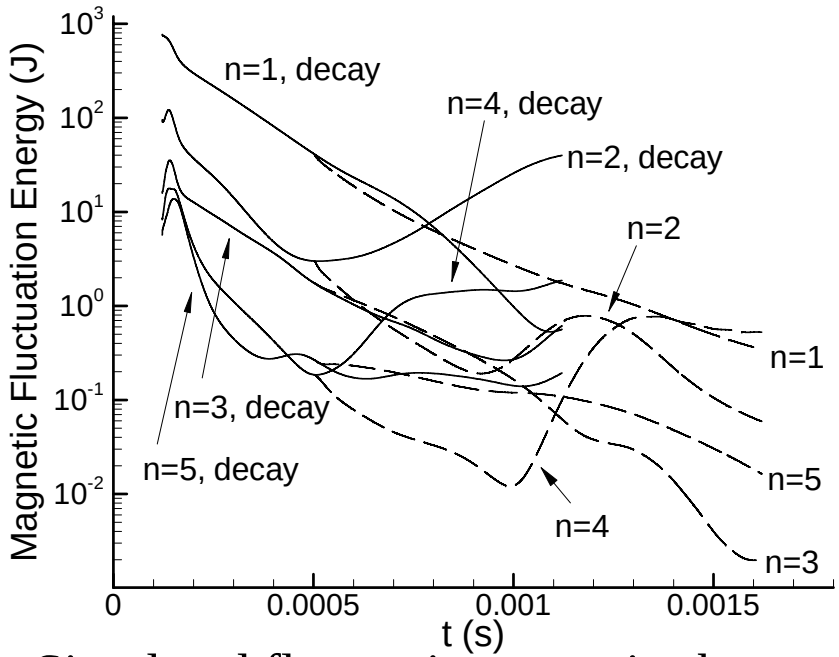

Simulated fluctuation energies by Fourier component with (dashed traces) and without (solid) the second current pulse.

- The second current pulse forces fluctuations to smaller amplitude and postpones the emergence of the *n*=2 mode.
- A simulation without the second current pulse shows much larger fluctuation levels, particularly in the *n*=2 component.

Plasma temperature within a toroidally shaped region increases significantly as the magnetic fluctuation level is reduced.

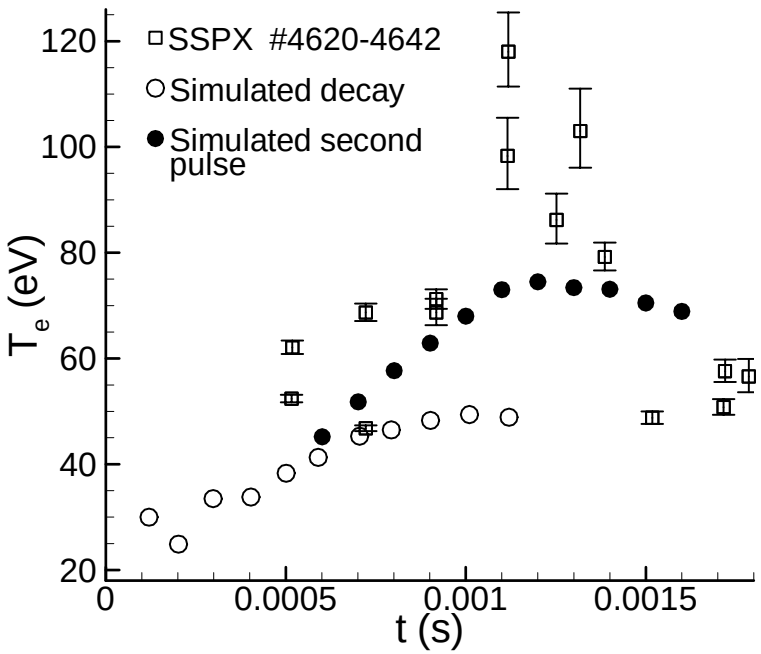

Comparison of temperatures measured with Thomson scattering in SSPX and simulation results with and without the second current pulse.

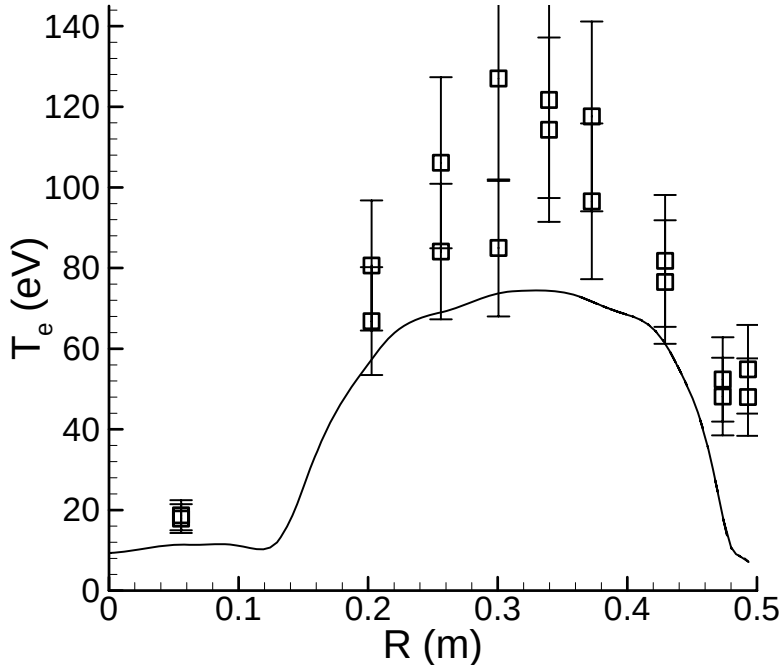

Profiles of midplane temperatures from SSPX (at 1.1 ms) and the simulation with the second current pulse (at 1.2 ms).

- The less dramatic response in the simulation may be due to limitations in the collisional transport model as confinement improves.
- The simulation response of 76 eV is also substantial, however. Without the second pulse, the peak temperature is only 49 eV.

Poincaré surfaces of section prove that the magnetic field develops structure, including flux surfaces, during the quiescent phase.

- During formation, the magnetic field shows chaotic scattering as also seen in 0-β simulations of sustained conditions [Finn *et al.*, PRL **85**, 4538 (2000)].

- Beginning with the current ramp-down after formation, open field lines lengthen, and a closed toroidal structure forms during the quiescent phase.

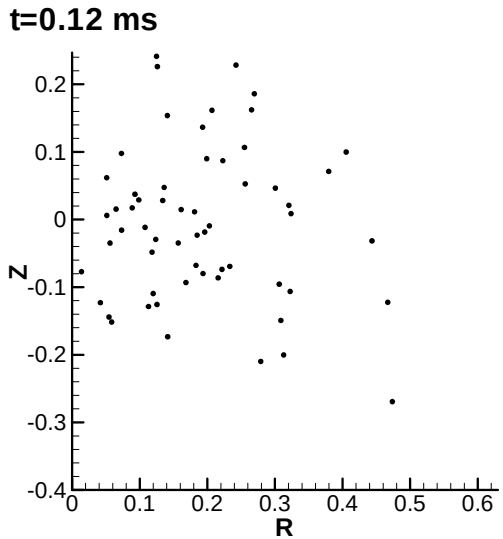

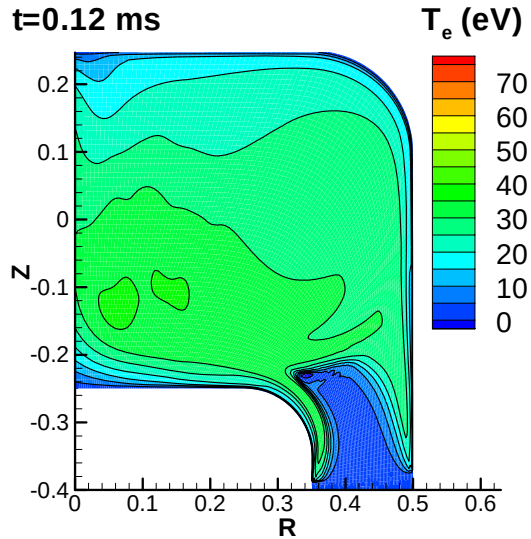

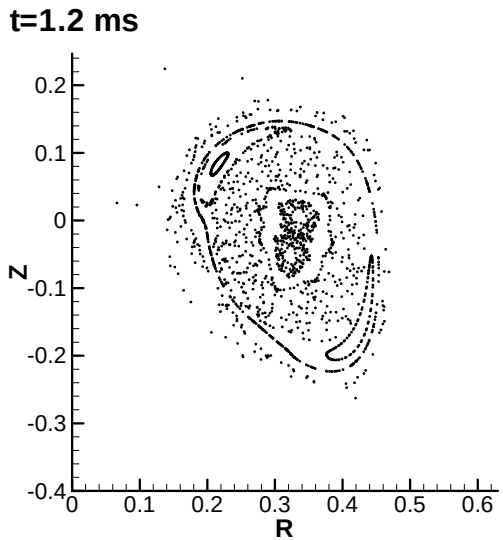

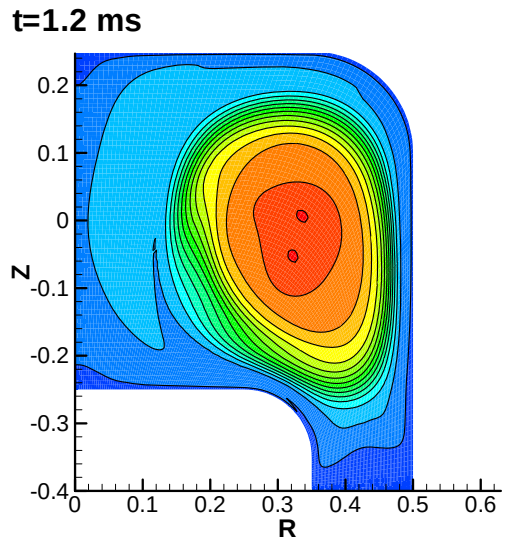

The second current pulse keeps the *q*-profile from falling significantly below 1/2, thereby reducing the impact of the (m=1,n=2) and (m=2,n=4) perturbations.

Safety factor profiles, computed as

$$q = \frac{d\langle\Phi\rangle}{d\langle\Psi\rangle}$$

in the amplified-flux region, show that the second current pulse maintains a flatter *q*-profile.

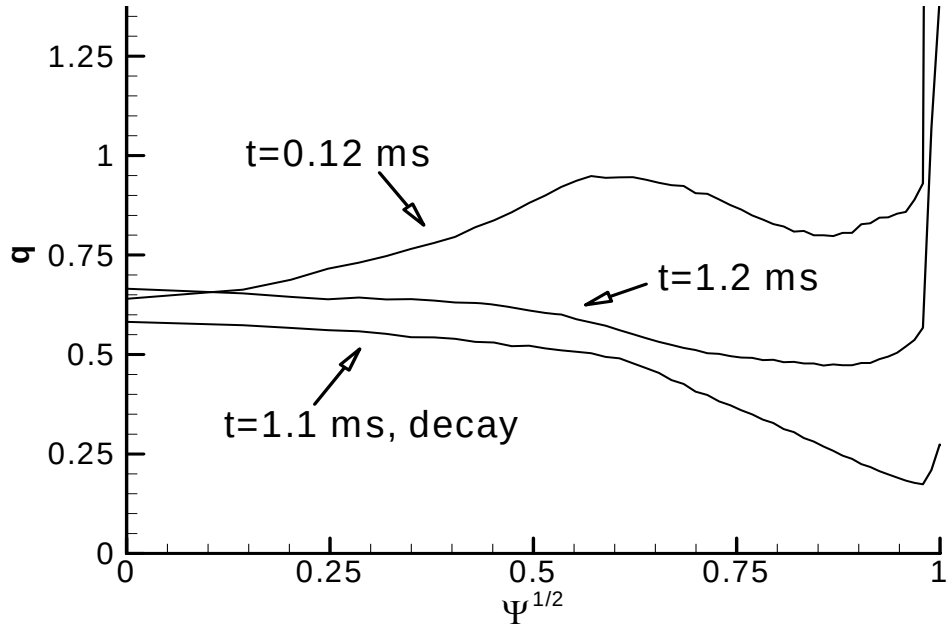

• The correspondence of MHD activity and resonances in MHD equilibria fitted to SSPX measurements has been noted [Woodruff *et al*. BAPS **48**, 150 (2003)].

Importance of Transients

• Although the second pulse injects half of the current of the formation pulse, dynamo activity is orders of magnitude smaller.

Here we consider the dynamo power density $-\langle \mathbf{v}\times\mathbf{b}\rangle\cdot\langle \mathbf{J}\rangle$

which contributes to the rhs of

$$\frac{1}{2\mu_0}\frac{\partial\langle B\rangle^2}{\partial t}+\nabla\cdot\langle \mathbf{E}\rangle\times\langle \mathbf{B}\rangle=-\langle \mathbf{E}\rangle\cdot\langle \mathbf{J}\rangle$$

At the center of the amplified flux region:

	$\langle \mathbf{v}\times\mathbf{b}\rangle\cdot\langle \mathbf{J}\rangle$	$\eta\langle \mathbf{J}\rangle^2$
Formation	1×10^9 W/m^3	2×10^7 W/m^3
Quiescent Phase	$\sim10^5$ W/m^3	3×10^6 W/m^3

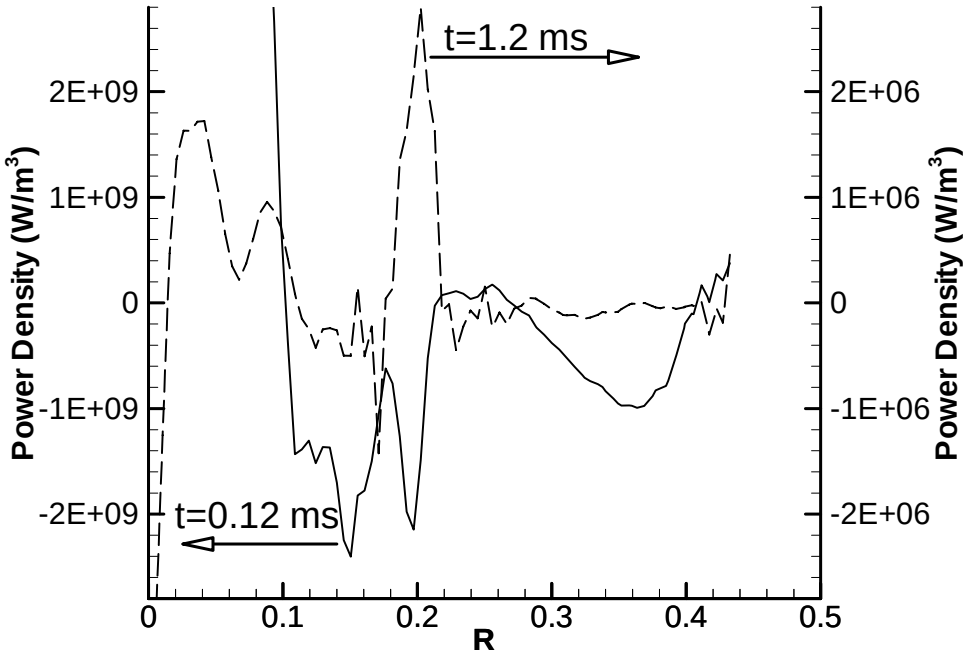

Dynamo power density along the midplane during formation and during the quiescent phase.

• Without any drive, the symmetric current would require ~8 ms to decay resistively at 50 eV.

• The quiescent phase with closed flux surfaces is not representative of sustainment.

Simulation of PPCD in MST

- We start from a saturated resistive MHD simulation of a cylindrical RFP with R/a=3, S=2000, and $0 \le n \le 42$.
- The first PPCD computation is 'old' PPCD: a poloidal **E** pulse.
  - The pulse is scaled to remove the same fraction of toroidal magnetic flux in the same number of tearing times as in MST.

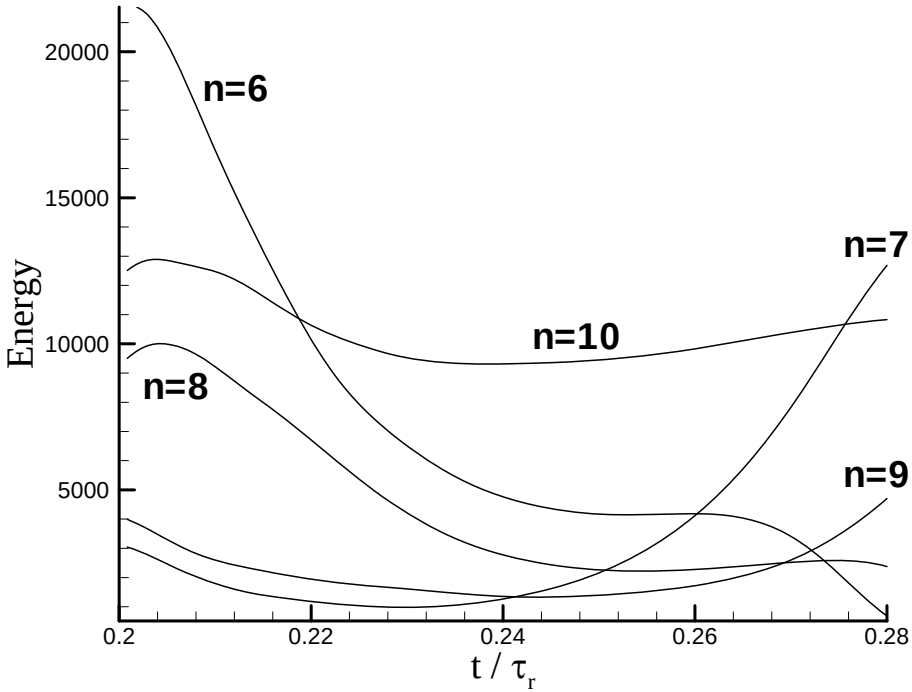

Magnetic Fluctuation Energies During E_θ Pulse

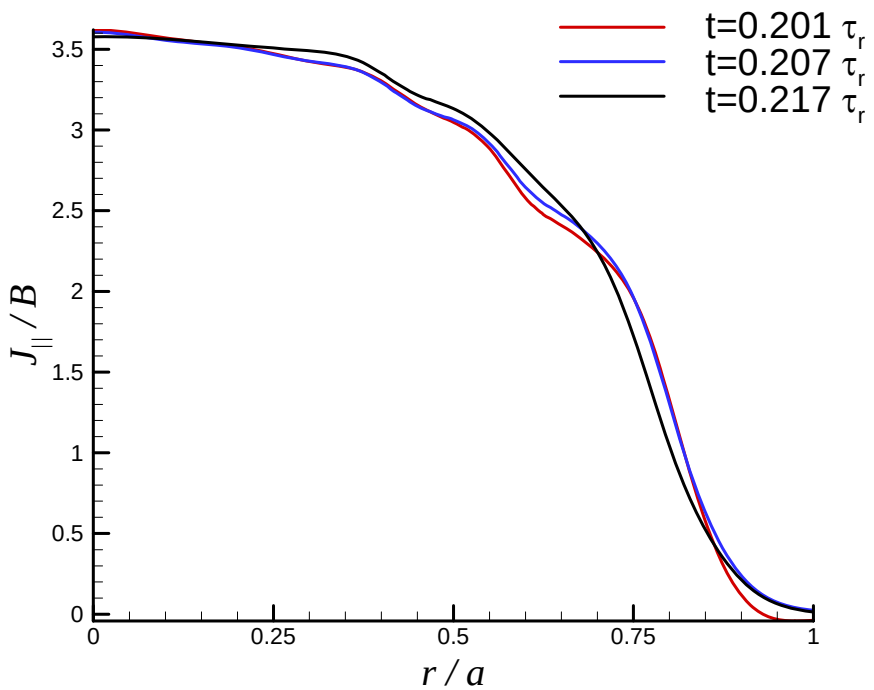

Initial Evolution of Parallel Current

To understand the prompt response of the core-resonant n=6, we have investigated linear stability properties of the evolving equilibrium.

- A computation of the mode's power exchange with the evolving equilibrium + dissipation indicates the same initial trend as the fluctuation energy.

$$-\mathrm{Re}\left\{\int\left[\langle\mathbf{J}\rangle\cdot\left\langle\tilde{\mathbf{v}}_n^*\times\tilde{\mathbf{b}}_n\right\rangle+\langle\mathbf{V}\rangle\cdot\left\langle\tilde{\mathbf{j}}_n^*\times\tilde{\mathbf{b}}_n\right\rangle+\eta\tilde{\mathbf{j}}_n^*\cdot\tilde{\mathbf{j}}_n+\rho\nu\left(\nabla\tilde{\mathbf{v}}_n^*\right)^T:\nabla\tilde{\mathbf{v}}_n\right]dVol\right\}$$

- Profiles of the power density do not clarify how the stabilization occurs, so we turn to Newcomb's equation & check $\Delta' = -\psi_s'(r_s)\psi_c(a)/\psi_s(a)$

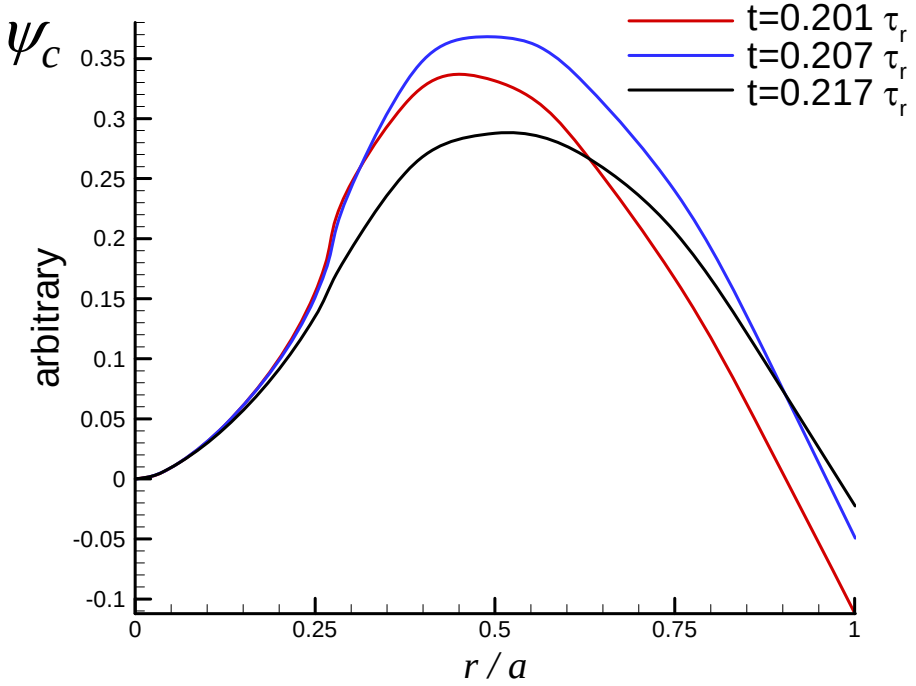

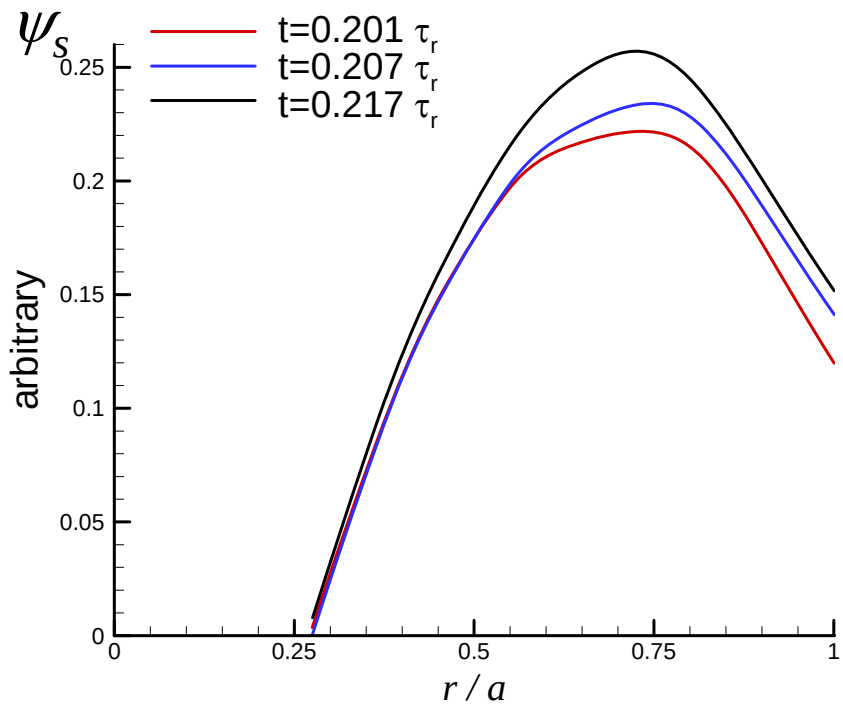

- **Changes in the solutions occur promptly in the core and are stabilizing.**

A computation with E-axial reduced during the E-poloidal pulse shows a longer period of magnetic fluctuation reduction.

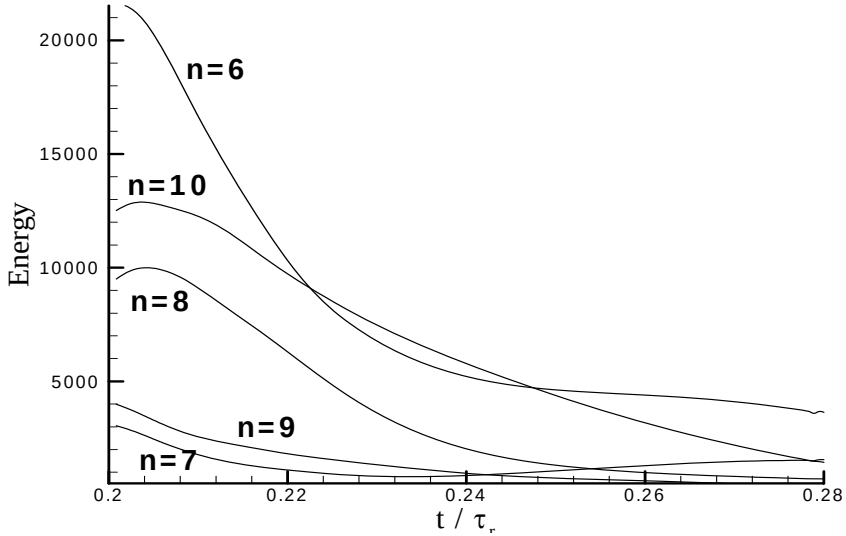

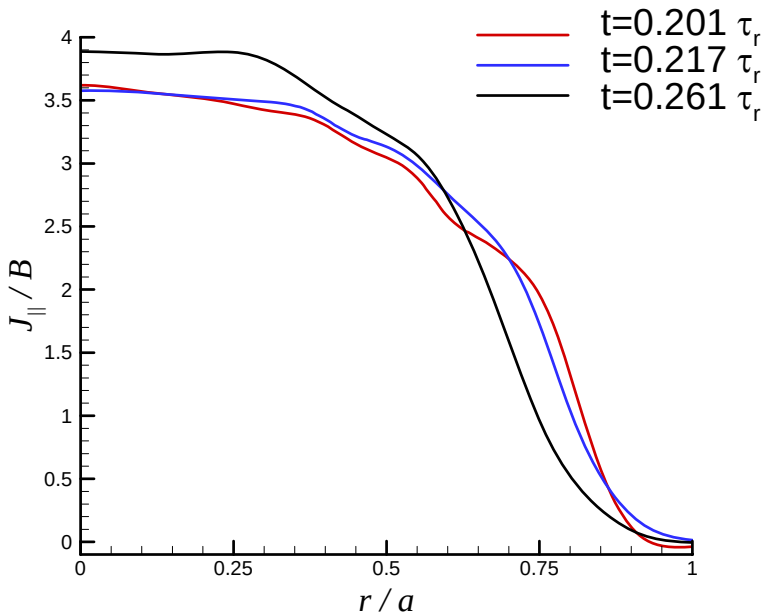

Parallel Current Maintaining E_z

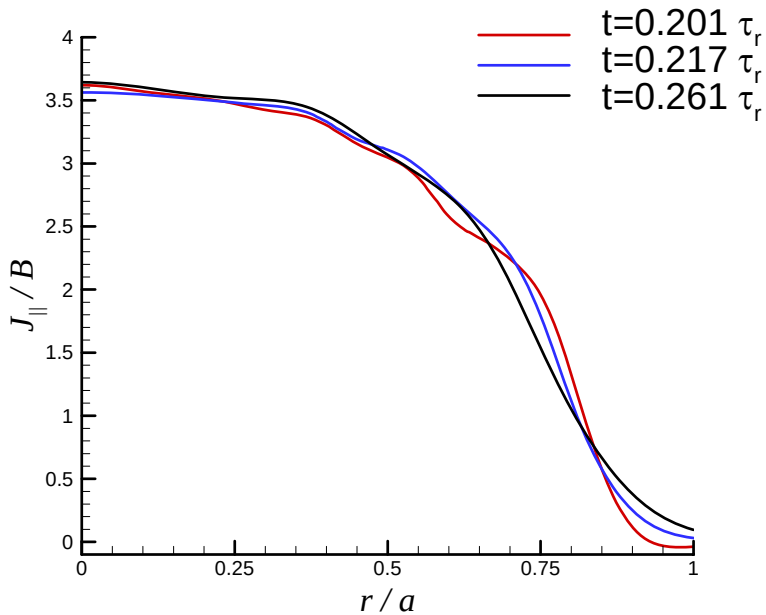

Parallel Current Reducing E_z

• Reducing axial-E keeps the pinch [Puiatti, NF] from overshooting the stable profile.

Comparison of Spheromak and PPCD Transients

- Aligning the axial direction of an electrostatically driven spheromak with the toroidal direction of an RFP makes a useful analogy.
  - The spheromak n=1 mode of the open-field current is similar to the m=1 dynamo modes of the RFP.
  - In both cases, fluctuations are driven by parallel current gradients associated with strong pinching. ($J_{||}/B$ is much larger than in tokamaks).
- The spheromak decay transient is analogous to reducing the RFP loop voltage.
  - The source of free energy is removed in both cases.
  - In the spheromak, the open field rapidly cools leading to an excessive loss of toroidal flux from the edge. The second current pulse in SSPX keeps the decay balanced.
  - Although there is no analogous drive in the spheromak, we note that the poloidal-**E** in RFP PPCD makes a prompt stabilizing contribution.

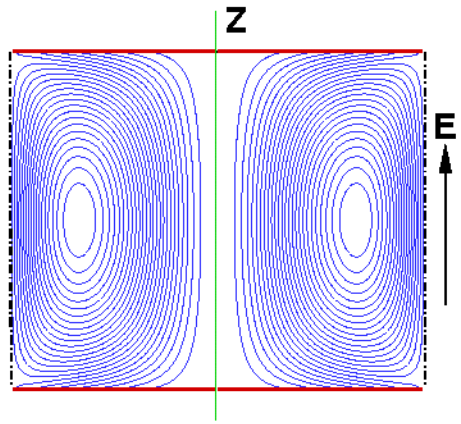

Flux-core Spheromak

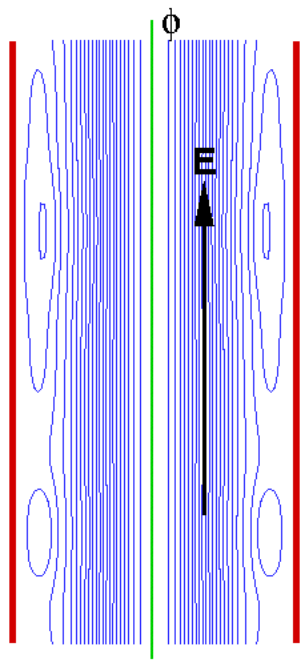

Cylindrical RFP

Conclusions

- Transients play a crucial role in spheromak experiments; thus, modeling injector current programming is necessary for detailed comparison of theory and experiment.
- The SSPX simulations find that the second current pulse is important for tailoring the current profile during decay, but it does not sustain the configuration [Sovinec, PRL **94** 35003 (2005)].
- PPCD in RFPs is known to induce transient effects. Simulations show that the poloidal-**E** pulse promptly increases parallel current in the interior, but reducing loop voltage prevents excessive pinching.
- That PPCD is able to maintain a favorable parallel current density profile lends support to the idea of a self-similar RFP ramp-down [Nebel, PoP **9**, 4968 (2002).]
- As in driven conditions, there are analogies between the spheromak and RFP transients.

Acknowledgments

- Bruce Cohen and Bick Hooper: collaboration on SSPX simulation studies
- Harry McLean: SSPX data
- Ken Fowler: relevance of collisional closures
- John Sarff, Brett Chapman and the MST group: PPCD discussions
- NIMROD Team: code development collaboration